CrossMark

Invariant and energy analysis of an axially retracting beam

Yang Xiaodong [a,*], Liu Ming [a], Zhang Wei [a], Roderick V.N. Melnik [b]

[a] *Beijing Key Laboratory of Nonlinear Vibrations and Strength of Mechanical Engineering, College of Mechanical Engineering, Beijing University of Technology, Beijing 100124, China*
[b] *M2NeT Laboratory, The MS2Discovery Interdisciplinary Research Institute, Wilfrid Laurier University, Waterloo, ON N2L 3C5, Canada*

Abstract   The mechanism of a retracting cantilevered beam has been investigated by the invariant and energy-based analysis. The time-varying parameter partial differential equation governing the transverse vibrations of a beam with retracting motion is derived based on the momentum theorem. The assumed-mode method is used to truncate the governing partial differential equation into a set of ordinary differential equations (ODEs) with time-dependent coefficients. It is found that if the order of truncation is not less than the order of the initial conditions, the assumed-mode method can yield accurate results. The energy transfers among assumed modes are discussed during retraction. The total energy varying with time has been investigated by numerical and analytical methods, and the results have good agreement with each other. For the transverse vibrations of the axially retracting beam, the adiabatic invariant is derived by both the averaging method and the Bessel function method.

1. Introduction

The dynamics of a flexible body such as a slender beam or string whose length changes with time has received a good deal of attention in recent years as one of the examples of the time-varying parameter systems. It leads to a typical model of axial moving system which is important in many areas of applications such as spacecraft antennae, elevator cables,[1] band saw blades,[2] paper sheet processing in high-speed copy machines,[3] and others.

The motion of a thin steel plate that is coiled in high-speed automatic coiling machines is an important application that sometimes leads to a violent vibration. Since the original works in this field,[4] such nonlinear dynamic motion has been formed as the spaghetti problem. To study this problem, Carrier[4] used a linear string theory to solve the corresponding eigenvalue problem with a time-varying boundary condition. Sugiyama et al.[5] presented a modeling method and an experimental procedure for the mechanism analysis of the spaghetti problem. In

their study, the effect of the transport velocity and the clearance were demonstrated, and the cause of a significant increase in the flexible body vibration was discussed from an energy balance viewpoint. The so called spaghetti and reverse spaghetti problems were also studied by Kobayashi and Watanabe.[6] They used a mechanical model and experiments to study the dynamic behavior of a flexible beam that was pulled into and drawn out of a gap in an elastic wall with a constant velocity. Mansfield and Simmonds[7] studied the motion of a sheet of paper in high-speed copy machines as an application of such problem.

The earlier detailed research of the deploying or retracting beam was presented by Tabarrok et al.[8] who derived nonlinear equations of motion of a beam with changing length and presented a closed-form similarity solution and a semi-analytic solution. It is known that the gyroscopic terms can be neglected in the model only for the case of low axial velocity. Tadikonda and Baruh[9] presented the analytical investigation of such a model without the effect of the gyroscopic terms. A finite element model of the axially moving beam based on a geometrically nonlinear beam formulation was studied by Downer and Park,[10] where the varying length of a beam was implemented by applying a moving finite element reference grid. They also formulated the equations of motion using the Hamilton principle. Kalaycioglu and Misra[11] presented approximate analytical solutions which were obtained for the transverse oscillations of deploying or retracting appendages of beam and tether types. Matsuzaki et al.[12] provided experimental data on bending oscillations of a deploying or retrieving beam cantilevered by a clamping device and formulated a finite element analysis for treating the corresponding oscillations. Behdinan and Tabarrok[13] used the updated Lagrangian and the co-rotational finite element methods to obtain the solutions for the geometrically non-linear flexible sliding beam. Tang et al.[14] studied the dynamics of variable-length satellite tethers using a flexible multi-body dynamics method. In their study, the governing equations of the tethers were derived using a new hybrid Eulerian and Lagrangian framework. Tang and Chen[15] investigated the nonlinear free transverse vibration of an in-plane moving plate with constant speed. The governing equation with the boundary conditions was derived from the Hamilton principle and the Hooke's law, and the method of multiple scales was employed to analyze the resulting nonlinear partial differential equation.

Zhu and Ni[16] discussed the energy of vibrations of a translating medium with variable length. Stabilization of a translating medium with variable length requires suppression of both the energy of vibration of a shortening medium and the amplitude of the response of a lengthening medium. Because the boundedness of the displacement did not ensure the boundedness of the energy for a time-varying system, Cooper[17] investigated the dynamic stability from the energy standpoint. Wang et al.[18] analyzed the energy transferred between the transverse vibration and the axial motion, concluding that the material viscosity helped stabilize the transverse vibration in both extension and retraction modes. Chen and Zhao[19,20] proposed a conserved quantity in the studying of axially moving beams and strings. Chen et al.[21] used the energy-like conserved quantity to verify the Layapunov stability of the straight equilibrium configuration of the axially moving material.

The construction of conserved quantity has the potential to reveal the physical interpretation of the non-conservative sys-tem. Although the energy-like invariants have been studied in the time-independent parameter systems as shown in Refs.[18–20], the conserved quantity analysis has not been found in the time-varying parameter system. To address the lack of this aspect, the authors discuss the mechanism and the dynamic characteristics of a slender beam that retracts from a prismatic joint. The transfers of energy among different modes are investigated numerically. The construction of adiabatic invariants by the averaging method and the application of the Bessel function method demonstrate the mechanism of the retracting beam. For the first order truncated system, the variation of total energy for transverse vibrations is presented by both analytical and numerical methods.

2. Governing equation

The physical configuration of the retracting beam is given in Fig. 1. The beam is retracted in the prismatic joint under the action of axial force F. The moving uniform beam area moment of inertia I, elastic modulus E, mass per unit length m_s, length $L(t)$, and retracting velocity $U(t)$ at time t are used in this research. Viewing the sliding beam as a system of changing mass, one assumes that the part of the beam inside the prismatic joint is non-deformable and has a prescribed axial motion. Along all length of the beam, the axial velocity is uniform since the beam is assumed inextensible. The Euler–Bernoulli beam model is used to determine the transverse motion of the beam described by $Y = Y(X, t)$ in plane as it is retracted from a finite length L_0.

We use three equations, namely, continuity equation, rotational equilibrium equation, and translational equilibrium equation, to derive the governing equation by studying the small segment of the beam as shown in Fig. 2 where M_1 and M_2 denote bending moment, F_1 and F_2 general force that includes the axial and shear force, and r_1 and r_2 radius vector.

Since the beam is inextensible, the mass per unit length of the projection on the X-axis is

$$m = m_s\sqrt{[1 + (\partial Y/\partial X)^2]} \tag{1}$$

The conservation of mass of a segment of the beam requires

$$\frac{d}{dt}\int_{X_1(t)}^{X_2(t)} m\,dx = U(t)m(X_2, t) - U(t)m(X_1, t) + \int_{X_1(t)}^{X_2(t)} \frac{\partial m}{\partial t}\,dx = 0 \tag{2}$$
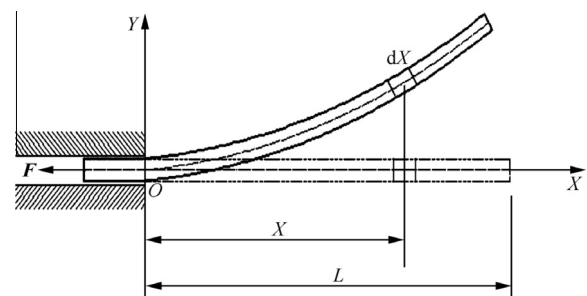

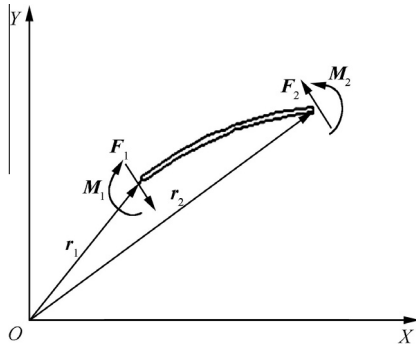**Fig. 1** Model of a retracting cantilever beam.

Fig. 2   End forces on a segment of beam.

which leads to

$$\frac{\partial}{\partial X}(mU) + \frac{\partial m}{\partial t} = 0 \tag{3}$$

Note that in Eq. (2), the following relation has been used:

$$\frac{dX_1}{dt} = \frac{dX_2}{dt} = U(t) \tag{4}$$

By Newton's second law, rotational equilibrium of the segment can be obtained as

$$M_2 - M_1 + (r_2 \times F_2) - (r_1 \times F_1) = \frac{d}{dt}\left(\int_{X_1(t)}^{X_2(t)} mr \times W dX\right) \tag{5}$$

where $r = iX + jY + k0$ is the radius vector and $W = dr/dt = iU + jV + k0$ the velocity vector. The i, j, k denote the unit vectors of X, Y, Z axes and U, V denote the velocities of X, Y directions respectively.

The left-hand side of Eq. (5) can be rewritten compactly as

$$M_2 - M_1 + (r_2 \times F_2) - (r_1 \times F_1)$$
$$= \int_{X_1(t)}^{X_2(t)} \frac{\partial}{\partial X}(M + r \times F)dX \tag{6}$$

With the help of Eq. (4), the right-hand side can be cast into

$$\frac{d}{dt}\left(\int_{X_1(t)}^{X_2(t)} mr \times W dX\right) = \int_{X_1(t)}^{X_2(t)} \frac{\partial}{\partial X}(mUr \times W)dX$$
$$+ \int_{X_1(t)}^{X_2(t)} \frac{\partial}{\partial t}(mr \times W)dX \tag{7}$$

Substituting Eqs. (6) and (7) into Eq. (5), one finds the rotational equilibrium:

$$\frac{\partial}{\partial t}(mr \times W) + \frac{\partial}{\partial X}(mUr \times W) = \frac{\partial}{\partial X}(M + r \times F) \tag{8}$$

For the translational equilibrium of the beam segment, the momentum theorem can be used to obtain

$$\int_{X_1(t)}^{X_2(t)} \frac{\partial F}{\partial X}dX = F_2 - F_1 = \frac{d}{dt}\int_{X_1(t)}^{X_2(t)} mW dX \tag{9}$$

Hence, the equation of translational equilibrium is

$$\frac{\partial}{\partial t}(mW) + \frac{\partial}{\partial X}(mUW) = \frac{\partial F}{\partial X} \tag{10}$$

Using Eq. (3), the rotational equilibrium and translational equilibrium equations (Eqs. (8) and (10)) can be written simply as

$$m\frac{d}{dt}(r \times W) = \frac{\partial}{\partial X}(M + r \times F) \tag{11}$$

$$m\frac{dW}{dt} = \frac{\partial F}{\partial X} \tag{12}$$

where the material derivative for the axially sliding beam is defined as

$$\frac{d}{dt} = \frac{\partial}{\partial t} + U\frac{\partial}{\partial X} \tag{13}$$

Substituting Eq. (13) into Eqs. (11) and (12) and rewriting the results in their component form yield

$$m\frac{dU}{dt} = \frac{\partial F_x}{\partial X} \tag{14}$$

$$m\frac{dV}{dt} = \frac{\partial F_y}{\partial X} \tag{15}$$

$$\frac{\partial M}{\partial X} = -F_y + F_x\frac{\partial Y}{\partial X} \tag{16}$$

where F_x and F_y are the components of F in the X and Y directions, and M is the magnitude of M in the Z direction. Note that transverse velocity for one point on the sliding beam is

$$V = \frac{dY}{dt} = \frac{\partial Y}{\partial t} + U\frac{\partial Y}{\partial X} \tag{17}$$

The axial force T and the shear force S are used in the analysis instead of F. Note that on the free end, the axial force T and the shear force S are zero. The transformation relations, based on Fig. 3, can be found as

$$\begin{cases} F_x = T\cos\theta - S\sin\theta \\ F_y = T\sin\theta + S\cos\theta \end{cases} \tag{18}$$

where θ is the angle between the X axis and the tangent to the beam. The following approximate relations can be applied:

$$\begin{cases} \cos\theta = 1 \\ \sin\theta = \frac{\partial Y}{\partial X} \end{cases} \tag{19}$$

The constitutive relation adopted in the current study is the moment curvature relation for the beam:

$$M = EI\frac{\partial^2 Y}{\partial X^2} \text{ or } S = -EI\frac{\partial^3 Y}{\partial X^3} \tag{20}$$
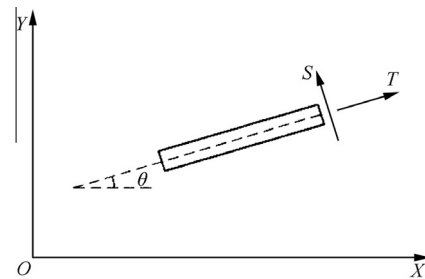

Fig. 3   Geometric diagram of coordinate transformation.

Substituting Eq. (18) into Eq. (14) and integrating the final result in the domain $[X, L]$ yield

$$T - S\frac{\partial Y}{\partial X} = -m(L - X)\frac{\mathrm{d}U}{\mathrm{d}t} \tag{21}$$

Substituting Eq. (18) into Eq. (15) and using Eq. (21), one obtains the partial differential equation with time-varying coefficients (since length L is varying with time) governing the transverse vibration of the sliding beam:

$$m\left[\frac{\partial^2 Y}{\partial t^2} + 2U\frac{\partial^2 Y}{\partial X\partial t} + U^2\frac{\partial^2 Y}{\partial X^2} + \frac{\mathrm{d}U}{\mathrm{d}t}\cdot\frac{\partial Y}{\partial X}\right]$$
$$= -EI\frac{\partial^4 Y}{\partial X^4} + m\left[\frac{\partial Y}{\partial X} - (L - X)\frac{\partial^2 Y}{\partial X^2}\right]\frac{\mathrm{d}U}{\mathrm{d}t} \tag{22}$$

The assumed-mode method[8,11] is an efficient way to solve the time-varying parameter differential equation. We express the transverse displacement $Y(X, t)$ in terms of a series of time-dependent mode functions of vibrations in generalized coordinates as

$$Y(X, t) = \sum_{i=1}^{\infty} f_i(t)\,\varphi_i(X, L) \tag{23}$$

where f_i denote the temporal generalized coordinates, and the assumed-mode functions φ_i denote spatial variables. Since L is a function of time, φ_i are time-dependent. The expressions for the eigenfunctions have the following form:

$$\varphi_i(X, L) = \frac{1}{\sqrt{L}}\left[\cosh\frac{\lambda_i X}{L} - \cos\frac{\lambda_i X}{L} - \alpha_i\left(\sinh\frac{\lambda_i X}{L} - \sin\frac{\lambda_i X}{L}\right)\right] \tag{24}$$

where

$$\alpha_i = \frac{\cos\lambda_i + \cosh\lambda_i}{\sin\lambda_i + \sinh\lambda_i} \tag{25}$$

and the eigenvalues λ_i are the roots of the transcendental equation

$$1 + \cos\lambda_i\cosh\lambda_i = 0 \tag{26}$$

Substituting Eqs. (23) and (24) into Eq. (22) and applying the Galerkin's procedure, one can write the truncated set of n ordinary differential equations (ODEs) in the following form:

$$\ddot{\boldsymbol{f}} + 2\left(\frac{U}{L}\right)\boldsymbol{A}\dot{\boldsymbol{f}} + \left[\frac{\dot{U}}{L}\boldsymbol{A} - \frac{U^2}{L^2}(\boldsymbol{A} + \boldsymbol{B}) + \boldsymbol{\Lambda}\right]\boldsymbol{f} = \boldsymbol{0} \tag{27}$$

where the vectors and matrices are defined as

$$\begin{cases} \boldsymbol{f} = [f_1 \quad f_2 \quad \cdots \quad f_n] \\ \Lambda_{ij} = \frac{EI}{\rho AL^4}\lambda_i^4\delta_{ij} \\ A_{ij} = \int_0^1(1 - \eta)\,\phi_i\phi_j'\mathrm{d}\eta - \frac{1}{2}\delta_{ij} \\ B_{ij} = \int_0^1(1 - \eta)^2\phi_i'\phi_j'\mathrm{d}\eta - \frac{1}{4}\delta_{ij} \\ \phi_i = \cosh(\lambda_i\eta) - \cos(\lambda_i\eta) - \alpha_i[\sinh(\lambda_i\eta) - \sin(\lambda_i\eta)] \\ i, j = 1, 2, \ldots, N \end{cases} \tag{28}$$

where ρ is the density of unit length of beam, A cross sectional area of beam, δ_{ij} Kronecker delta, and $\eta = X/L$.

3. Transient response to initial conditions

The time-varying parameter system Eq. (27) is integrated using a Runge–Kutta algorithm with error control. In the computation, the mass per unit length m_s is chosen as 0.599 kg/m, and stiffness $EI = 3798$ N·m^2, which have been used in Ref.[8]

3.1. Truncation order analysis

First, we check the accuracy of the assumed-mode truncation method with different truncation order n by the following computational example. The initial conditions are assumed as

$$[f_1 \quad f_2 \quad \cdots \quad f_n \quad \dot{f}_1 \quad \dot{f}_2 \quad \cdots \quad \dot{f}_n]_{t=0}$$
$$= [0.1 \quad 0.1 \quad 0.2 \quad 0 \quad \cdots \quad 0] \tag{29}$$

The first three order assumed-modes are given values, while the others are set to zero.

Based on the 1, 2, 3, and 7 order assumed-mode truncation method, the transient response of the tip deflection is presented in Fig. 4 for different retracting velocities with initial length $L_0 = 3$ m. The dot-dashed line denotes the tip deflection with time for the case of the 1-order truncation, $n = 1$; the dashed line denotes that for the 2-order truncation, $n = 2$; and the solid line denotes that for the 3-order and 7-order truncations, $n = 3, 7$. The 1-order truncation gives a smooth deflection curve, which is caused by the first order initial condition $f_1 = 0.1$. The 2-order truncation describes the superposed response to the first and second order initial conditions. In
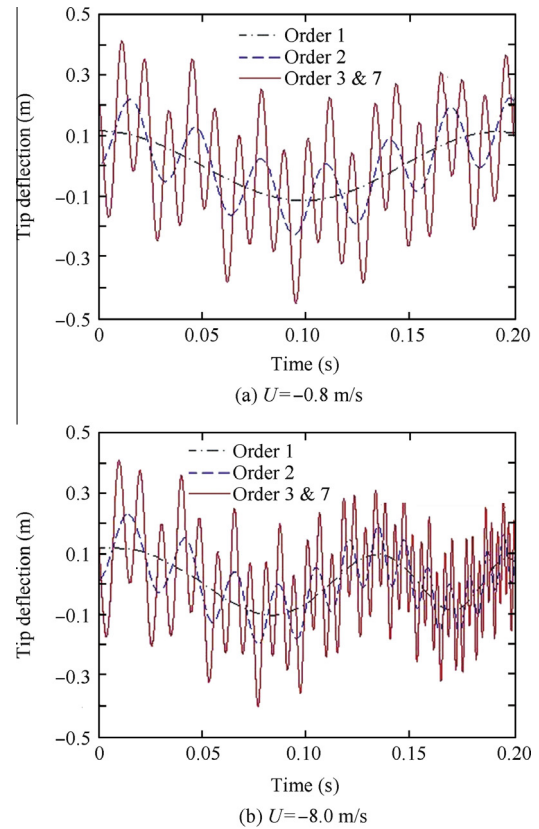

Fig. 4 Tip deflection response for the first 3 order initial conditions for $L_0 = 3$ m.

order to make the graphics more clear, the corresponding curves for $n = 4, 5, 6$ are not marked in Fig. 4. It can be found that the truncation order higher than 3 can predict the transient tip deflection response very well to the combination of the first three initial modes, for both high and low retracting velocities.

3.2. Energy variation among different modes of vibration

Since Eq. (27) is a set of coupled time-varying ODEs, we cannot study the energy of the assumed-mode analytically.

A numerical method will be used instead to study the variation of the generalized coordinates f, which denote the amplitudes of the assumed-modes. By using the Runge–Kutta method, the responses of all the assumed-modes can be determined under different initial conditions.

Now, we consider the solutions for the first order initial condition problem

$$[f_1 \quad f_2 \quad \ldots \quad f_7 \quad \dot{f}_1 \quad \dot{f}_2 \quad \ldots \quad \dot{f}_7]_{t=0} = [0.1 \quad 0 \quad 0 \quad \ldots \quad 0] \tag{30}$$
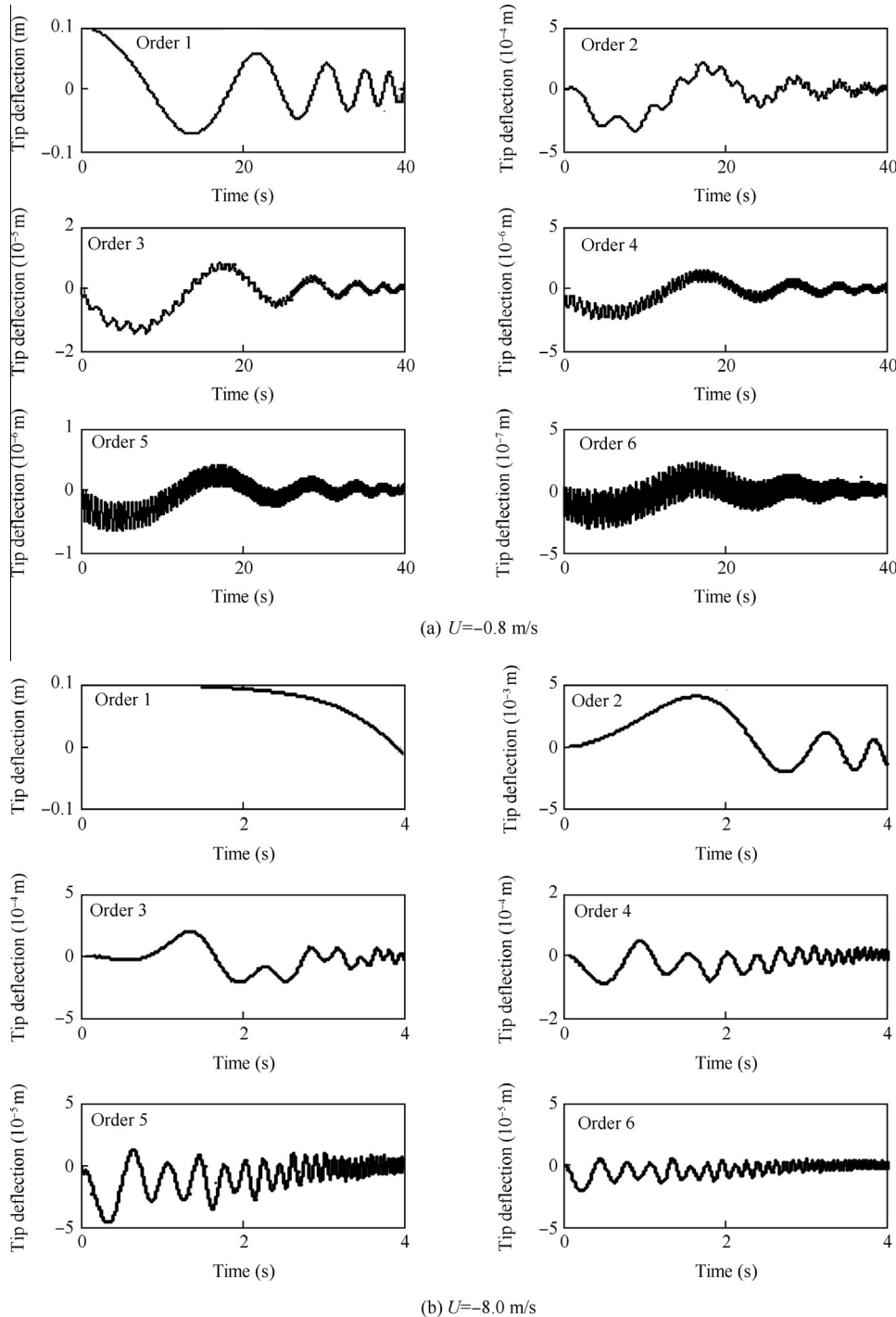

(a) $U=-0.8$ m/s

(b) $U=-8.0$ m/s

Fig. 5   The first six mode responses to initial mode of Order 1.

where the first mode initial generalized coordinate is nonzero, while the other mode initial generalized coordinates and all initial generalized velocities are zero. In order to achieve more accurate results, we take 7-order truncation for Eq. (27). The response of the first six modes determined by the first order initial mode is presented in Fig. 5.

It can be found from the plots of Fig. 5 that the amplitude of the first order assumed-mode decreases gradually with time from the beginning, while the other modes show high amplitudes at first and then the amplitudes for each mode decrease. Hence, it can be concluded that although the system is excited by the first order initial condition, the energy is transferred to the other modes during the retraction.

The plots in Figs. 6 and 7 present the responses of the first six modes due to the second and third order initial conditions, respectively. This phenomenon explains that the energy due to the initial condition can spread to other vibration modes, which is impossible in the time-independent linear systems. From Figs. 6 and 7 it can be found that the modes much closer to the initial mode obtain more energy than those far away. From Fig. 5 to Fig. 7, the energy transfers among different modes for two kinds of velocities are presented. By inspection of the plots
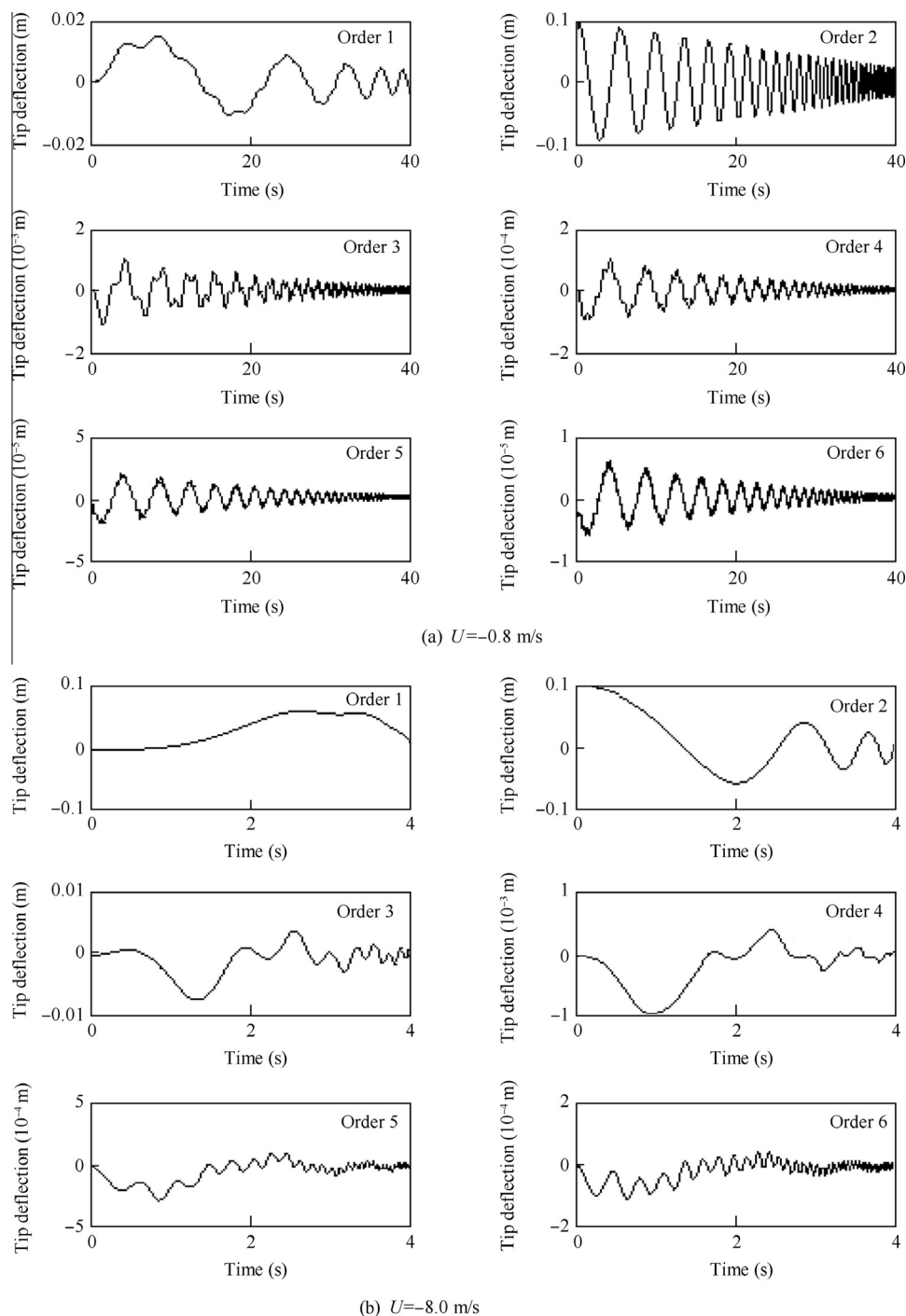

(a) $U=-0.8$ m/s

(b) $U=-8.0$ m/s

Fig. 6 The first six mode responses to initial mode of Order 2.

in Figs. 5–7, it can be found that the energy transferred from the initial mode to the other modes for higher retraction velocity is much stronger than that for lower retraction velocity.

From the Eq. (27), the velocity dependent term $-(A + B) \times U^2/L^2$ can explain the phenomenon of the energy transfers. The matrix A is skew symmetric while the matrix B is symmetric. So the nondiagonal matrix $A + B$ can lead to the coupling of different vibration modes.

4. Invariant of retracting beam

In this section, the adiabatic invariant is constructed by both the averaging method and the Bessel function method. Since the accuracy of the first order truncation can be satisfied in finite retracting time if the velocity is set slow, the first order truncation will be used in the study of the mechanism of the retracting beam.

4.1. Invariant by averaging method

The dynamics in the first order truncation of the time-varying parameter system will be studied here by the averaging method. Let $n = 1$, and the Eq. (27) becomes

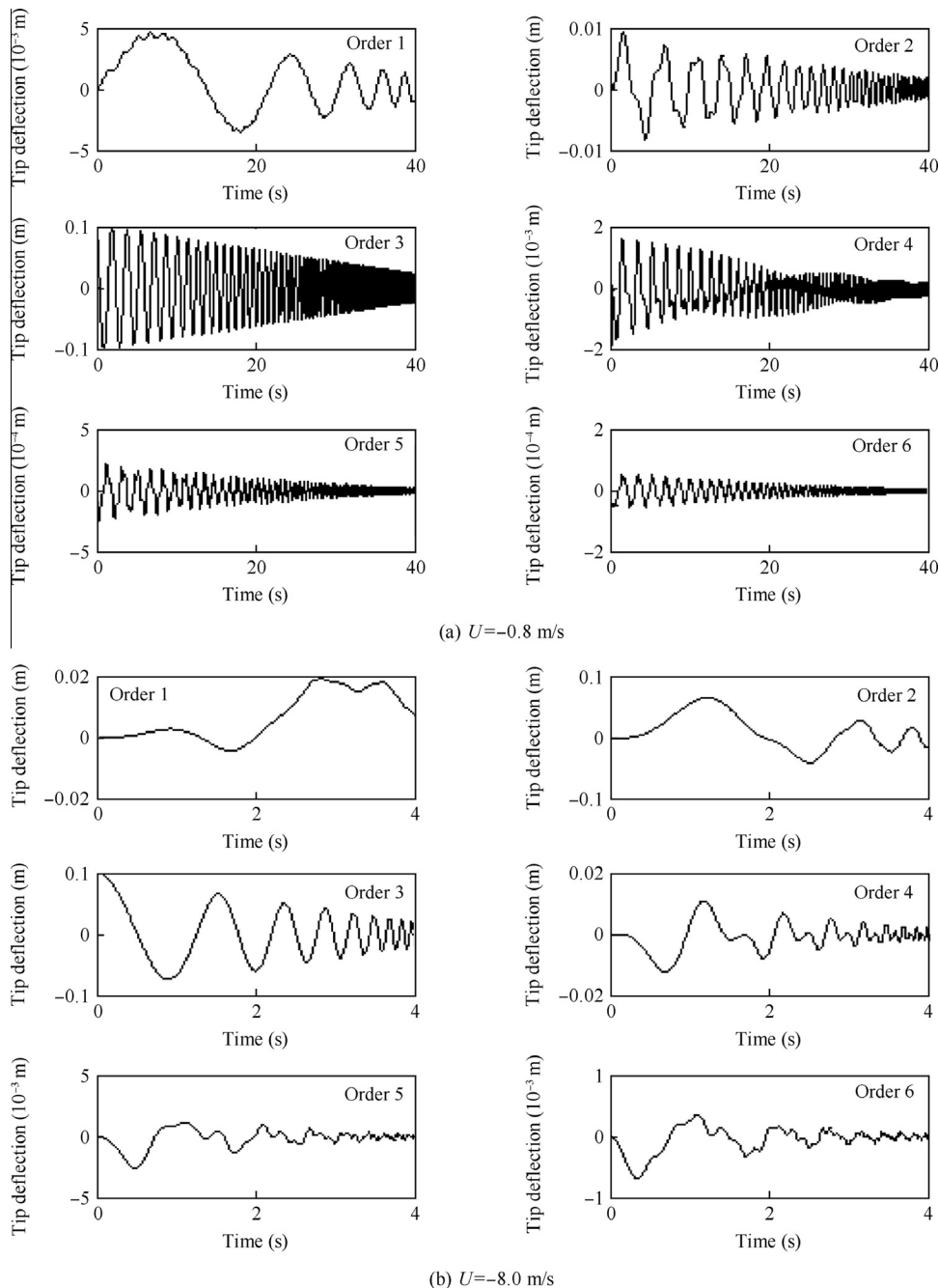$$\ddot{f}_1 + \left(-\frac{U^2}{L^2}B_{11} + \Lambda_{11}\right)f_1 = 0 \tag{31}$$

(a) $U = -0.8$ m/s

(b) $U = -8.0$ m/s

Fig. 7   The first six mode responses to initial mode of Order 3.

where B_{11} and Λ_{11} are presented in Eq. (28).

Since $B_{11} \ll \Lambda_{11}$, for low retracting velocity, i.e., $-(U^2/L^2)B_{11} \ll \Lambda_{11}$, Eq. (31) can be written as

$$\ddot{f}_1 + \omega^2(t) f_1 = 0 \tag{32}$$

where the instantaneous frequency is expressed as

$$\omega^2(t) = -\frac{U^2}{L^2} B_{11} + \Lambda_{11} \tag{33}$$

Now we introduce the averaging method to transform the form of Eq. (32), put $\dot{f}_1 = \omega(t) g_1$ and set

$$\begin{cases} f_1 = r \sin\varphi \\ g_1 = r \cos\varphi \end{cases} \tag{34}$$

Substituting Eq. (34) and their derivatives into Eq. (32), we obtain

$$\begin{cases} \dot{r} = -\dfrac{r}{\omega(t)} \cdot \dfrac{d\omega}{dt} \cos^2\varphi \\[2mm] \dot{\varphi} = \omega(t) + \dfrac{1}{\omega(t)} \cdot \dfrac{d\omega(t)}{dt} \sin\varphi \cos\varphi \end{cases} \tag{35}$$

By integrating the right-hand side of the first equation of Eq. (35) with respect to φ over $[0, 2\pi]$, we obtain

$$r^2 \omega(t) = c \tag{36}$$

where c is the integral constant.

By considering Eqs. (34) and (36), we find

$$\omega(t) f_1^2 + \frac{1}{\omega(t)} \dot{f}_1^2 = c \tag{37}$$

where constant c is determined by initial conditions. This relation is referred to as an adiabatic invariant for the time-varying structure, which has been studied earlier.[22] Here, we will demonstrate the adiabatic invariant obtained by the first order truncation by the numerical method.

(a) Phase obtained by numerical method

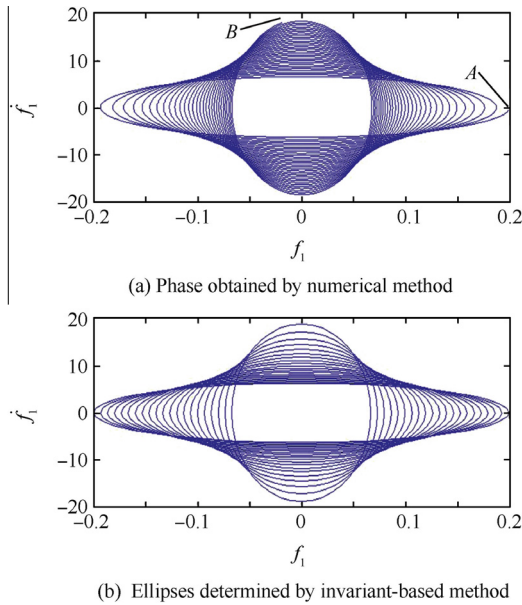
(b) Ellipses determined by invariant-based method

Fig. 8 Comparison of variables determined by numerical and invariant-based methods.

Fig. 8(a) presents the phase map calculated numerically with the Runge–Kutta method based on the 7-order truncation under the first order mode initial condition

$$[f_1 \quad f_2 \quad \cdots \quad f_7, \quad \dot{f}_1 \quad \dot{f}_2 \quad \cdots \quad \dot{f}_7]_{t=0}$$
$$= [0.2 \quad 0 \quad 0 \quad \cdots \quad 0] \tag{38}$$

In the computation, the initial length $L_0 = 3$ m, the initial velocity $U = -1$ m/s, and the time of retracting $t = 2$ s.

As shown in Fig. 8(a), the Point A is the starting point and the Point B is the end point based on the above initial condition. It can be found that the maximum transverse velocity is increasing and the maximum transverse deflection is decreasing with the retracting process. This phenomenon is caused by the fact that the instantaneous natural frequencies are increasing while the overall length shortens.

Based on the adiabatic invariant Eq. (37), we can obtain a series of ellipses depicted in Fig. 8(b) with the same initial conditions for every 0.1 s from $t = 0$ s to $t = 2$ s. The areas of every ellipse share the same value $2\pi/c$ as presented in Eq. (37). The isolated ellipses in Fig. 8(b) obtained by the adiabatic invariant have the same contour with the continuous phase map in Fig. 8 (b) obtained numerically. Hence, the adiabatic invariant can well describe the mechanism of the retracting beam vibrations.

4.2. Invariant by Bessel function method

When the beam retracts at constant axial velocity, its equation of vibration motion can be rewritten as

$$\ddot{\mathbf{f}} + 2\left(\frac{U}{L}\right)\mathbf{A}\dot{\mathbf{f}} + \left[-\frac{U^2}{L^2}(\mathbf{A}+\mathbf{B}) + \mathbf{\Lambda}\right]\mathbf{f} = \mathbf{0} \tag{39}$$

which can be obtained from Eq. (27) by setting $a = \dot{U} = 0$. The first order truncation for Eq. (39) is

$$\ddot{f}_1 + \left(\frac{0.25 - v^2}{t^2} + \frac{\beta^2}{t^4}\right)f_1 = 0 \tag{40}$$

where

$$\begin{cases} \beta^2 = \Lambda_{11}t^4 = \dfrac{EI\lambda_1^4}{\rho A L^4}t^4 \\[3mm] v^2 = B_{11} + 0.25 \end{cases} \tag{41}$$

When v is not a positive integer, the general solution to Eq. (40) is given by

$$f_1 = \sqrt{t}\left[D_1 J_v\left(\frac{\beta}{t}\right) + D_2 J_{-v}\left(\frac{\beta}{t}\right)\right] \tag{42}$$

where J is a Bessel function of Order v and the constants D_1 and D_2 depend on the initial conditions. The qualitative behavior of the retracting beam for small and large values of t can be determined by the asymptotic values of the Bessel function:

$$\begin{cases} t \to \infty, \quad \left(\dfrac{\beta}{t}\right) \to 0, \quad J_{\pm v} \to \dfrac{(\beta/2t)^{\pm v}}{\Gamma(1 \pm v)} \\[4mm] t \to 0, \quad \left(\dfrac{\beta}{t}\right) \to \infty, \quad J_{\pm v} \to \sqrt{\dfrac{2t}{\pi\beta}}\dfrac{\cos}{\sin}\left(\dfrac{\beta}{t} - \dfrac{\pi}{4} - \dfrac{v\pi}{2}\right) \end{cases} \tag{43}$$

where $\Gamma(\cdot)$ is the Gamma function. The asymptotic values imply that at the initial stage of the axial retracting, the oscillatory motions will be dominant. At a later stage, an unbounded motion will dominate the lateral motion.[8]

Considering the asymptotic condition when $t \to 0$, and substituting the second equation of Eq. (43) into Eq. (42), one obtains

$$f_1 = t\sqrt{\frac{2}{\pi\beta}}\left[D_1 \cos\left(\frac{\beta}{t} - \frac{\pi}{4} - \frac{v\pi}{2}\right) + D_2 \sin\left(\frac{\beta}{t} - \frac{\pi}{4} - \frac{v\pi}{2}\right)\right]$$

$$= \frac{t}{\sqrt{\beta}}C\cos\left(\frac{\beta}{t} + \psi\right) \tag{44}$$

where the constant C can be determined from the initial condition.

The first derivative of f_1 can be obtained approximately as

$$\dot{f}_1 = \frac{\sqrt{\beta}}{t}A\sin\left(\frac{\beta}{t} + \psi\right) \tag{45}$$

Combining Eqs. (44) and (45), we find

$$\frac{\beta}{t^2}f_1^2 + \frac{\dot{f}_1^2}{\beta/t^2} = c \tag{46}$$

By analyzing the result Eq. (33) obtained in the last subsection, we deduce that

$$\omega(t) = \sqrt{-\frac{U^2}{L^2}B_{11} + \Lambda_{11}}$$

$$= \sqrt{-\frac{B_{11}U^2}{(L_0 + Ut)^2} + \frac{EI\lambda^4}{m(L_0 + Ut)^4}} \approx \frac{\beta}{t^2} \tag{47}$$

It can be found that for a slow retracting axial velocity, $t \to 0$, $\omega(t) \to \beta/t^2$. We can conclude that the results obtained by the averaging method and those by the Bessel function agree well in the low velocity case.

5. Variation of total energy

In this section, the total energy varying with time has been investigated by numerical and analytical methods. The effect of high retracting velocity on the analytical results has been presented, and the relation between the total energy and the length of retracting has also been discussed.

5.1. Energy variation

Let $L = L_0 + Ut$, and then the energy based on the first order truncation can be obtained as

$$\begin{cases} E_k = \frac{1}{2}\dot{f}_1^2 \\ E_p = \frac{1}{2}\omega^2(t)f_1^2 \\ E_t = E_k + E_p = \frac{1}{2}\omega^2(t)f_1^2 + \frac{1}{2}\dot{f}_1^2 \end{cases} \tag{48}$$

where E_k denotes kinetic energy, E_p potential energy, and E_t total energy.

Considering Eq. (37), we can rewrite the third equation of the total energy in Eq. (48) as

$$E_t = \omega^2(t)f_1^2 + \dot{f}_1^2 = \omega(t)c \tag{49}$$

where

$$c = \frac{1}{2}f_1^2\omega(0) = \frac{1}{2}f_1^2\sqrt{-\frac{U^2}{L^2}B_{11} + \Lambda_{11}} \tag{50}$$

It can be concluded that the total energy is proportional to the instantaneous frequency of the system, which is valid for the first order truncated case. Furthermore, we will verify this result by comparing the analytical results with numerical data.

When the initial length of beam L_0 is 2 m, the retracting velocity U is 0.8 m/s and the time of retracting t is 0.5 s, the change of the energy E_t with the time-dependent length is plotted in Fig. 9. The dot lines denote the numerical solution, and
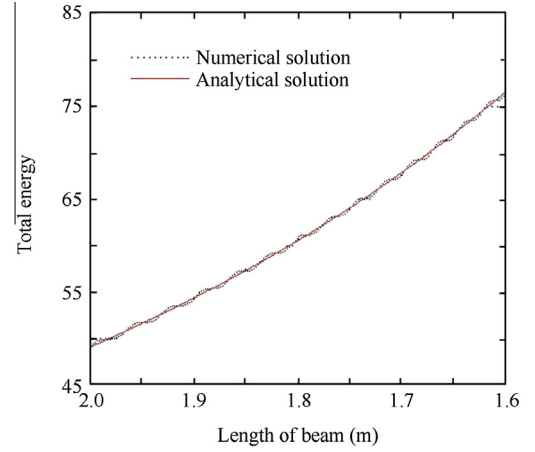

Fig. 9   Energy variation with length of beam.
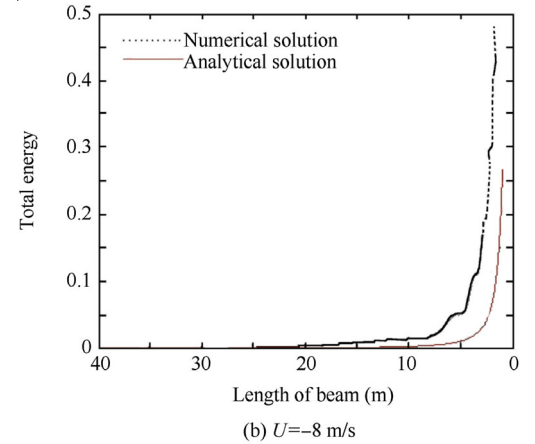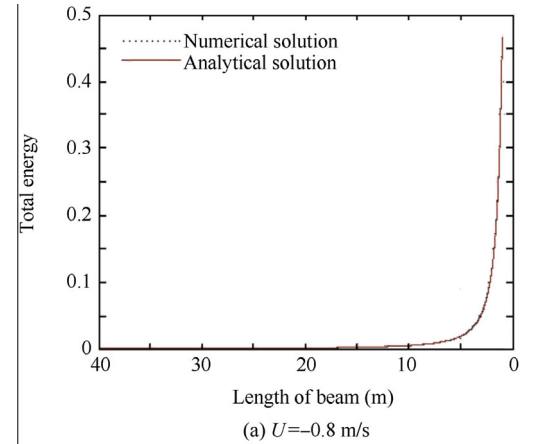

(a) $U=-0.8$ m/s

(b) $U=-8$ m/s

Fig. 10   Comparison between analytical solution and numerical solution for different retracting velocities.

the solid line denote the analytical solution of the first order truncated system. They have good agreement when compared to each other. It can be found that with the decreasing length of the beam, the energy is increasing. If the retracting velocity is zero, the system would be a general cantilever beam with constant length.

5.2. Effect of retracting velocity on analytical solution

It can be found that the analytical solution based on the first order truncation has higher accuracy in the earlier stage of retraction when the velocity is low. However, the accuracy will be lowered during the later stage of retracting when the initial length of the beam is long or the retracting velocity is high. Two energy variation diagrams for two different retracting velocities are presented in Fig. 10 where the dot lines denote the numerical solution and the solid lines denote the analytical solution. In the case of low retracting velocity as shown in Fig. 10(a), the analytical method yields good results. In the case of high retracting velocity as shown in Fig. 10(b), the analytical method provides results with less accuracy in the later stage of retracting process.

6. Conclusions

The mechanism of a retracting cantilevered beam has been investigated based on the assumed-mode truncation method by studying the energy and invariants of the system.

(1) The accuracy of the truncation method has been validated with numerical examples.
(2) The effect of the axial velocity on the transfer of the total energy of transverse vibration among assumed-modes has been analyzed.
(3) The adiabatic invariant, constructed by both the averaging method and the Bessel function method, provided a tool to explain the mechanism of the retracting beam.
(4) The variation of the total energy has been investigated by the first order truncated system. It has been found that the total energy is proportional to the instantaneous frequency, which has also been verified numerically.

Acknowledgements

References

1. Terumichi Y, Ohtsuka M, Yoshizawa M, Fukawa Y, Tsujioka Y. Nonstationary vibrations of a string with time-varying length and a mass-spring system attached at the lower end. *Nonlinear Dyn* 1997;**12**(1):39–55.

2. Mote Jr CD. A study of band saw vibrations. *J Franklin Inst* 1965;**279**(6):430–44.
3. Stolte J, Benson RC. Dynamic deflection of paper emerging from a channel. *ASME J Vib Acoust* 1992;**114**(2):187–93.
4. Carrier GF. The spaghetti problem. *Am Math Mon* 1949;**56**(10):669–72.
5. Sugiyama S, Kobayashi N, Komaki Y. Modeling and experimental methods for dynamic analysis of the spaghetti problem. *ASME J Vib Acoust* 2005;**127**(1):44–51.
6. Kobayashi N, Watanabe M. Dynamics and stability of spaghetti and reverse spaghetti problems coupled with fluid force. *Multibody Sys Dyn* 2004;**11**(2):111–25.
7. Mansfield L, Simmond JG. The reverse spaghetti problem: Drooping motion of an elastica issuing from a horizontal guide. *ASME J Appl Mech* 1987;**54**(1):147–50.
8. Tabarrok B, Leech CM, Kim YI. On the dynamics of an axially moving beam. *J Franklin Inst* 1974;**297**(3):201–20.
9. Tadikonda SSK, Baruh H. Dynamics and control of a translating flexible beam with a prismatic joint. *J Dyn Syst Meas Contr* 1992;**114**(3):422–7.
10. Downer JD, Park KC. Formulation and solution of inverse spaghetti problem: Application to beam deployment dynamics. *AIAA J* 1993;**31**(2):339–47.
11. Kalaycioglu S, Misra AK. Approximate solutions for vibrations of deploying appendages. *J Guidance* 1991;**14**(2):287–93.
12. Matsuzaki Y, Taki Y, Toyama M. Vibration of a cantilevered beam during deployment and retrieval: Analysis and experiment. *Smart Mater Struct* 1995;**4**:334–9.
13. Behdinan K, Tabarrok B. A finite element formulation for sliding beams, Part I. *Int J Numer Methods Eng* 1998;**43**(7):1309–33.
14. Tang JL, Ren GX, Zhu WD, Ren H. Dynamics of variable-length tethers with application to tethered satellite deployment. *Commun Nonlinear Sci Numer Simul* 2011;**16**(8):3411–24.
15. Tang YQ, Chen LQ. Nonlinear free transverse vibrations of in-plane moving plates: Without and with internal resonances. *J Sound Vib* 2011;**330**(1):110–26.
16. Zhu WD, Ni J. Energetics and stability of translating media with an arbitrarily varying length. *ASME J Vib Acoust* 2000;**122**(3):295–304.
17. Cooper J. Asymptotic behavior for the vibrating string with a moving boundary. *J Math Anal App* 1993;**174**(1):67–87.
18. Wang LH, Hu ZD, Zhong Z, Ju JW. Dynamic analysis of an axially translating viscoelastic beam with an arbitrarily varying length. *Acta Mech* 2010;**214**(3/4):225–44.
19. Chen LQ, Zhao WJ. The energetics and the stability of axially moving Kirchhoff string. *J Acoust Soc Am* 2005;**117**(1):55–8.
20. Chen LQ, Zhao WJ. A conserved quantity and the stability of axially moving nonlinear beams. *J Sound Vib* 2005;**286**(3):663–8.
21. Chen LQ, Lim CW, Ding H. Energetics and conserved quantity of an axially moving string undergoing three-dimensional nonlinear vibration. *Acta Mech Sin* 2008;**24**(2):215–21.
22. Verhulst F. *Nonlinear differential equations and dynamical systems.* 2nd ed. Berlin Heidelberg: Springer-Verlag; 1996. p. 147–9.

Yang Xiaodong is a professor in Beijing University of Technology. He received the Ph.D. degree in mechanics from Shanghai Institute of Applied Mathematics and Mechanics in 2004. His main research interests are vibration analysis of axially moving continuum, nonlinear dynamics and perturbation methods of nonlinear system.

Liu Ming is a graduate student of Beijing University of Technology. His main research interests are vibration analysis of axially moving continuum and perturbation method of nonlinear system.

Zhang Wei is a professor in Beijing University of Technology. He received the Ph.D. degree in mechanics from Tianjin University in 1997. His main research interests include nonlinear dynamics and global perturbation method of high dimensional nonlinear systems.